Exclusive lepton pair production in ultra-peripheral collisions

Jakub Wagner

Theoretical Physics Department
National Center for Nuclear Research, Warsaw

Exclusive and diffractive processes
in high energy proton-proton and nucleus-nucleus collisions
Trento, February 27th, 2012

in collaboration with
B. Pire (CPhT Ecole Polytechnique, Palaiseau) and L. Szymanowski (NCNR, Warsaw)

Outline

1. Introduction
   - Deep Inelastic Scattering
   - Exclusive processes
2. Generalized parton distributions
   - definition,properties, ...
3. Timelike Compton Scattering
   - Kinematics
   - Bethe-Heitler, TCS, Interference
   - Energy dependence
4. NLO TCS
   - factorization
   - DVCS Compton Form Factors
5. Ultraperipheral collisions

Deep Inelastic Scattering $e\,p \to e\,X$

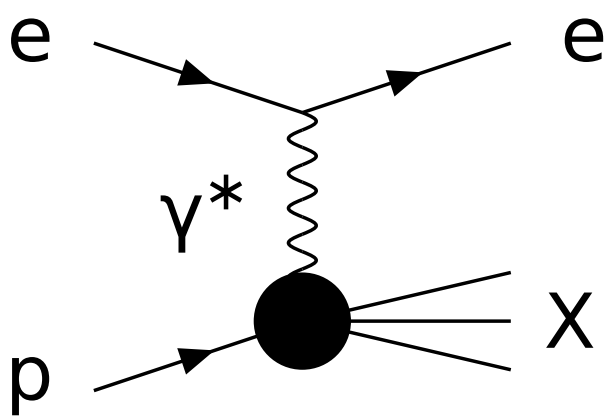

In the Björken limit i.e. when the photon virtality $Q^2 = -q^2$ and the squared hadronic c.m. energy $(p+q)^2$ become large, with the ratio $x_B = \frac{Q^2}{2p\cdot q}$ fixed, the cross section factorizes into a hard partonic subprocess calculable in the pertutbation theory, and a parton distributions.

DIS

- Parton distributions encode the distribution of longitudinal momentum and polarization carried by quarks, antiquarks and gluons within fast moving hadron
- Still not clear how nucleons and other hadrons are built from quarks and gluons
- PDFs don't provide infomation about how partons are distributed in the transverse plane and ...
- about how important is the orbital angular momentum in making up the total spin of the nucleon.
- Recently - growing interest in the exclusive scattering processes, which may shed some light on these issues through the generalized parton distributions (GPD).

DVCS
Kinematics

The simplest and best known process is Deeply Virtual Compton Scattering: $e\,p \to e\,p\,\gamma$

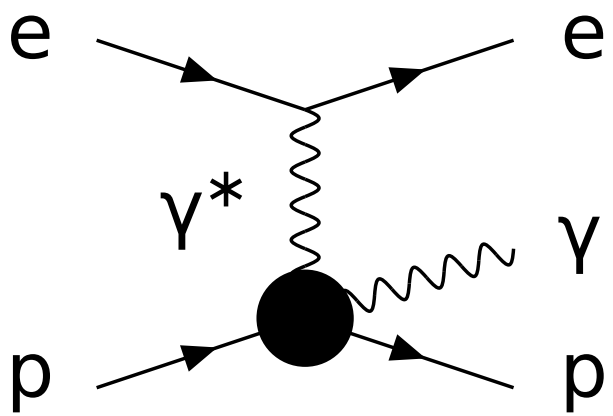

Factorization into GPDs and perturbative coefficient function - on the level of amplitude.

$$\text{DIS}: \quad \sigma = \text{PDF} \otimes \text{partonic cross section}$$
$$\text{DVCS}: \quad \mathcal{M} = \text{GPD} \otimes \text{partonic amplitude}$$

DVCS

Factorization - Generalized parton distributions

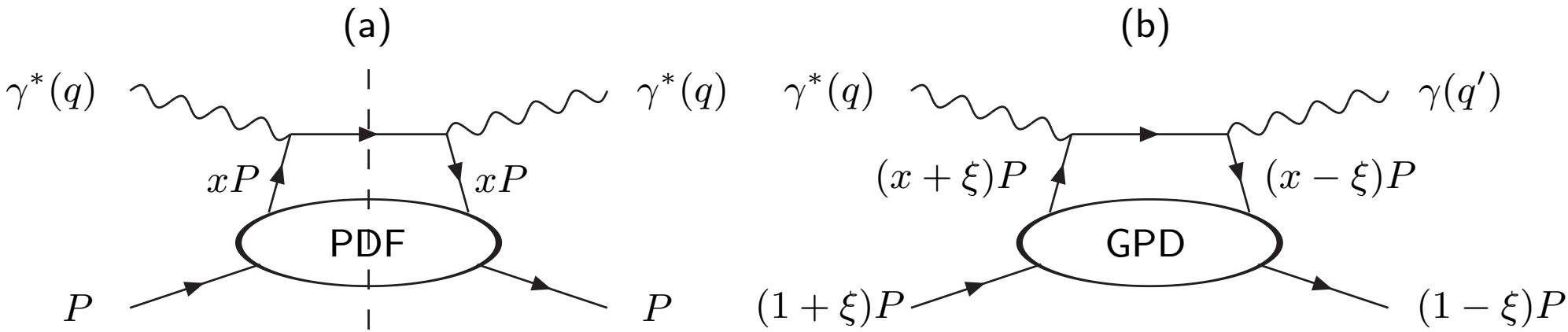

Figure: Deep Inelastic Scattering cross section is given by the imaginary part of diagram (a). Amplitude of Deeply Virtual Compton Scattering is given by diagram (b).

Experiments

- DESY - Hermes, H1, Zeus
- JLAB CLAS $6\,\mathrm{GeV} \rightarrow$ JLAB $12\,\mathrm{GeV}$
- Compass
- EIC
- RHIC/LHC

GPD definition.

$$
\begin{aligned}
F^q &= \frac{1}{2}\int \frac{dz^-}{2\pi}\, e^{ixP^+z^-} \langle p'|\, \bar{q}(-\frac{1}{2}z)\, \gamma^+ q(\frac{1}{2}z)\, |p\rangle \Big|_{z^+=0,\, \mathbf{z}=0} \\
&= \frac{1}{2P^+}\left[H^q(x,\xi,t)\, \bar{u}(p')\gamma^+ u(p) + E^q(x,\xi,t)\, \bar{u}(p')\, \frac{i\sigma^{+\alpha}\Delta_\alpha}{2m} u(p) \right], \\
F^g &= \frac{1}{P^+}\int \frac{dz^-}{2\pi}\, e^{ixP^+z^-} \langle p'|\, G^{+\mu}(-\frac{1}{2}z)\, G_\mu{}^+(\frac{1}{2}z)\ |p\rangle \Big|_{z^+=0,\, \mathbf{z}=0} \\
&= \frac{1}{2P^+}\left[H^g(x,\xi,t)\, \bar{u}(p')\gamma^+ u(p) + E^g(x,\xi,t)\, \bar{u}(p')\, \frac{i\sigma^{+\alpha}\Delta_\alpha}{2m} u(p) \right],
\end{aligned}
$$

- interpretation, ERBL, DGLAP

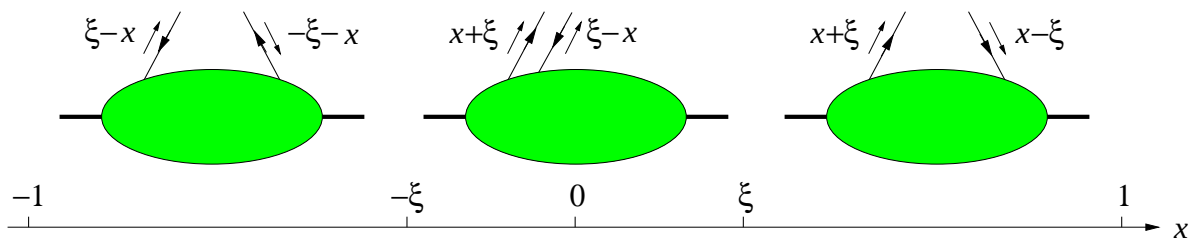

- Factorization scale dependance,
- Three variables x, ξ, t .

GPD - properties,

- Forward limit:

$$\begin{aligned} H^q(x,0,0) &= q(x)\,, \qquad \text{for} \qquad x>0\,, \\ H^q(x,0,0) &= -\bar{q}(x)\,, \qquad \text{for} \qquad x<0\,, \\ H^g(x,0,0) &= xg(x)\,, \end{aligned}$$

  similarly for polarized distributions and PDFs.

- Reduction to form factors:

$$\int_{-1}^{1} dx\, H^q(x,\xi,t) = F_1^q(t), \qquad \int_{-1}^{1} dx\, E^q(x,\xi,t) = F_2^q(t),$$

  where the Dirac and Pauli form factors

$$\langle p'|\,\bar{q}(0)\gamma^\mu q(0)\,|p\rangle = \bar{u}(p')\left[\,F_1^q(t)\,\gamma^\mu + F_2^q(t)\,\frac{i\sigma^{\mu\alpha}\Delta_\alpha}{2m}\,\right]u(p),$$

Ji sum rule.

Big attention to the GPD's because of the connection with a Ji sum rule:

$$\frac{1}{2} = \sum_q J_q + J_g$$

$$J_q = \frac{1}{2}[A_q(0) + B_q(0)], \qquad J_g = \frac{1}{2}[A_g(0) + B_g(0)], \tag{1}$$

and can be represented in terms of GPDs:

$$\begin{aligned} A_q(t) + B_q(t) &= \int_{-1}^{1} dx\, x\Big[H_q(x,\xi,t) + E_q(x,\xi,t)\Big], \\ A_g(t) + B_g(t) &= \int_{0}^{1} dx\, \Big[H_g(x,\xi,t) + E_g(x,\xi,t)\Big]. \end{aligned} \tag{2}$$

Kinematics of TCS

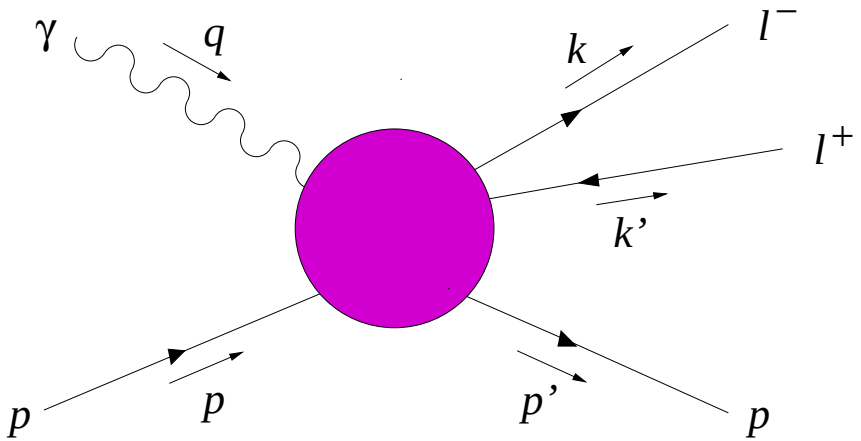

Figure: Real photon-proton scattering into a lepton pair and a proton.

$$\gamma(q)N(p) \to \gamma^*(q')N(p') \to l^-(k)l^+(k')N(p')$$

at small $t = (p' - p)^2$ and large *timelike* virtuality $(k + k')^2 = q'^2 = Q'^2$ of the final state dilepton, timelike Compton scattering (TCS), shares many features with DVCS.

Experiments: JLab (low energy), RHIC and LHC (ultraperipheral)

Coordinates

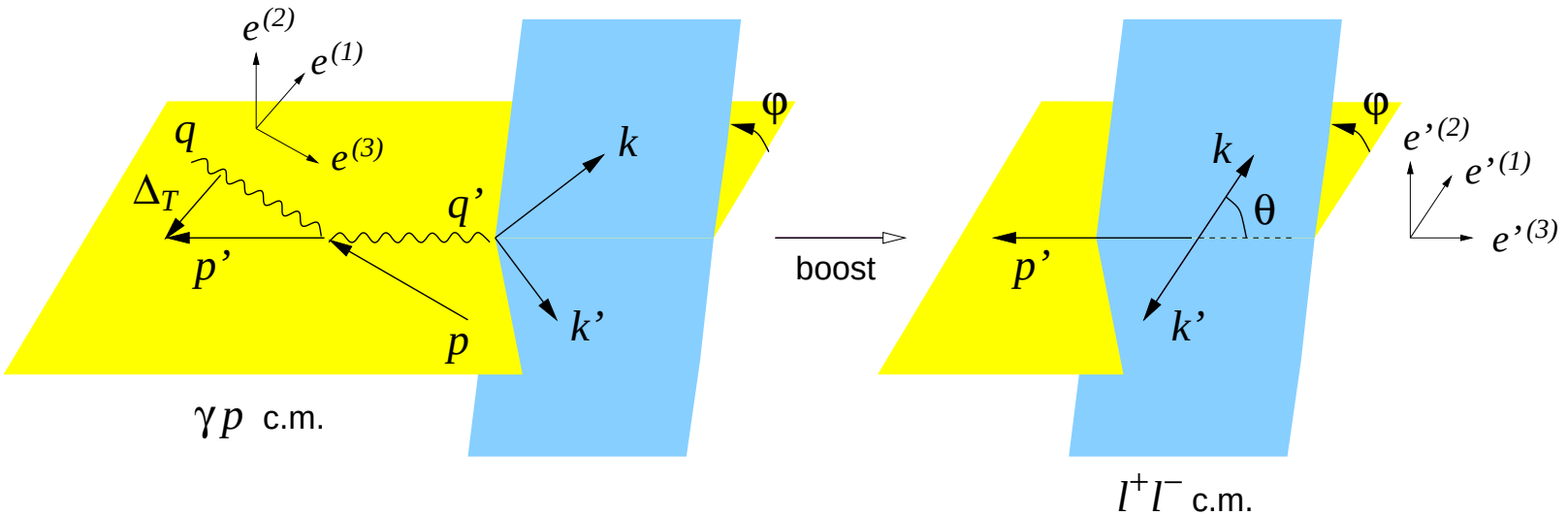

Figure: Kinematical variables and coordinate axes in the γp and $\ell^+\ell^-$ c.m. frames.

The Bethe-Heitler contribution

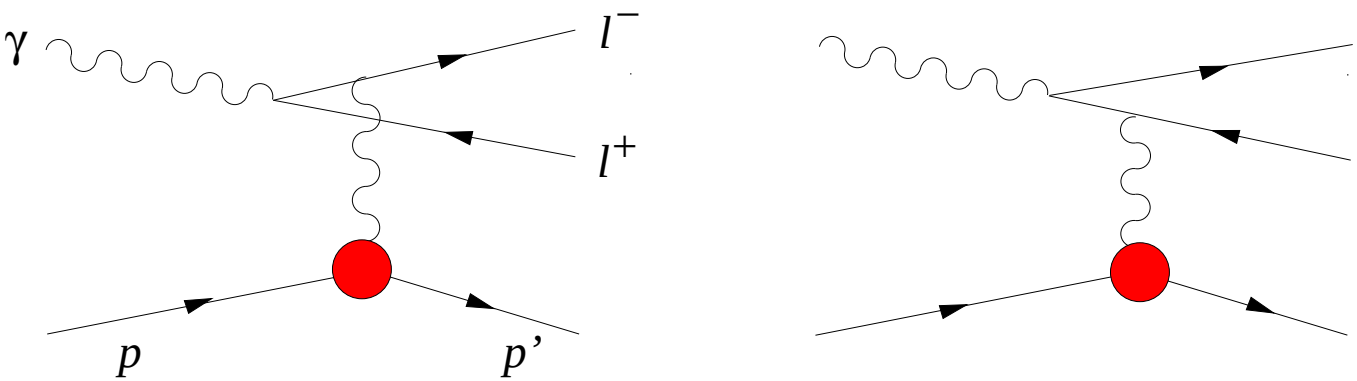

Figure: The Feynman diagrams for the Bethe-Heitler amplitude.

$$\frac{d\sigma_{BH}}{dQ'^2 dt d\cos\theta} \approx 2\alpha^3 \frac{1}{-tQ'^4} \frac{1+\cos^2\theta}{1-\cos^2\theta} \left(F_1(t)^2 - \frac{t}{4M_p^2} F_2(t)^2 \right),$$

For small θ BH contribution becomes very large

The Compton contribution

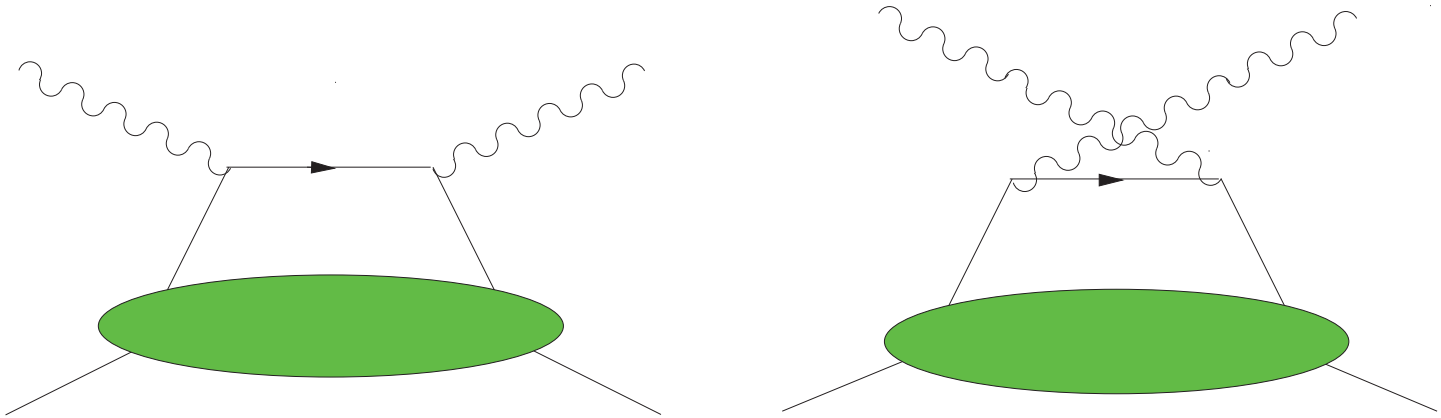

Figure: Handbag diagrams for the Compton process in the scaling limit.

$$\frac{d\sigma_{TCS}}{dQ'^2 d\Omega dt} \approx \frac{\alpha^3}{8\pi}\frac{1}{s^2}\frac{1}{Q'^2}\left(\frac{1+\cos^2\theta}{4}\right) 2(1-\xi^2)\,|\mathcal{H}|^2,$$

$$\mathcal{H}(\xi,t) \quad = \quad \sum_q e_q^2 \int_{-1}^{1} dx \left(\frac{1}{\xi - x + i\epsilon} - \frac{1}{\xi + x + i\epsilon}\right) H^q(x,\xi,t),$$

TCS at lower energies

Berger, Diehl, Pire, 2002

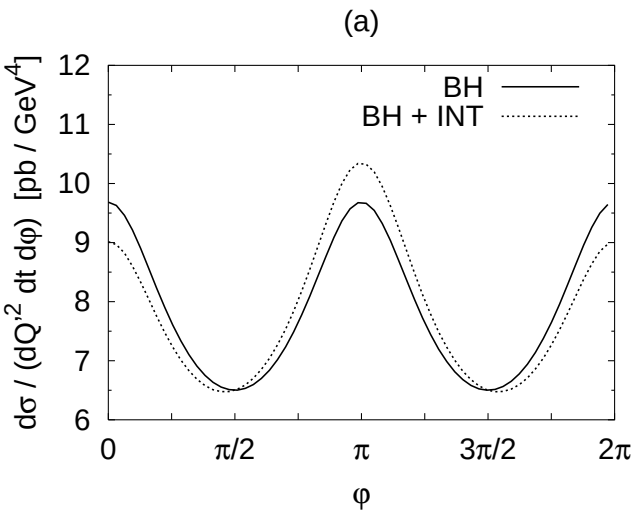

B-H dominant; TCS dominated by quark GPDs

Charge asymmetry $\sim$ interference of B-H and TCS

B-H cross section

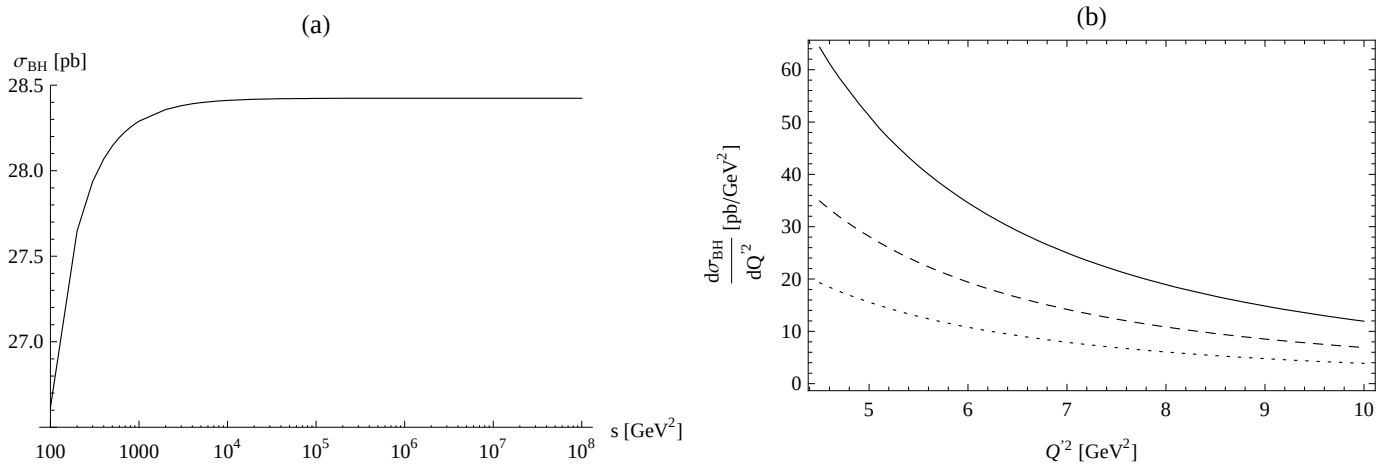

Figure: (a) The BH cross section integrated over $\theta \in [\pi/4, 3\pi/4]$, $\varphi \in [0, 2\pi]$, $Q'^2 \in [4.5, 5.5]\,\mathrm{GeV}^2$, $|t| \in [0.05, 0.25]\,\mathrm{GeV}^2$, as a function of γp c.m. energy squared s. (b) The BH cross section integrated over $\varphi \in [0, 2\pi]$, $|t| \in [0.05, 0.25]\,\mathrm{GeV}^2$, and various ranges of θ : $[\pi/3, 2\pi/3]$ (dotted), $[\pi/4, 3\pi/4]$ (dashed) and $[\pi/6, 5\pi/6]$ (solid), as a function of Q'^2 for $s = 10^5\,\mathrm{GeV}^2$

TCS cross section

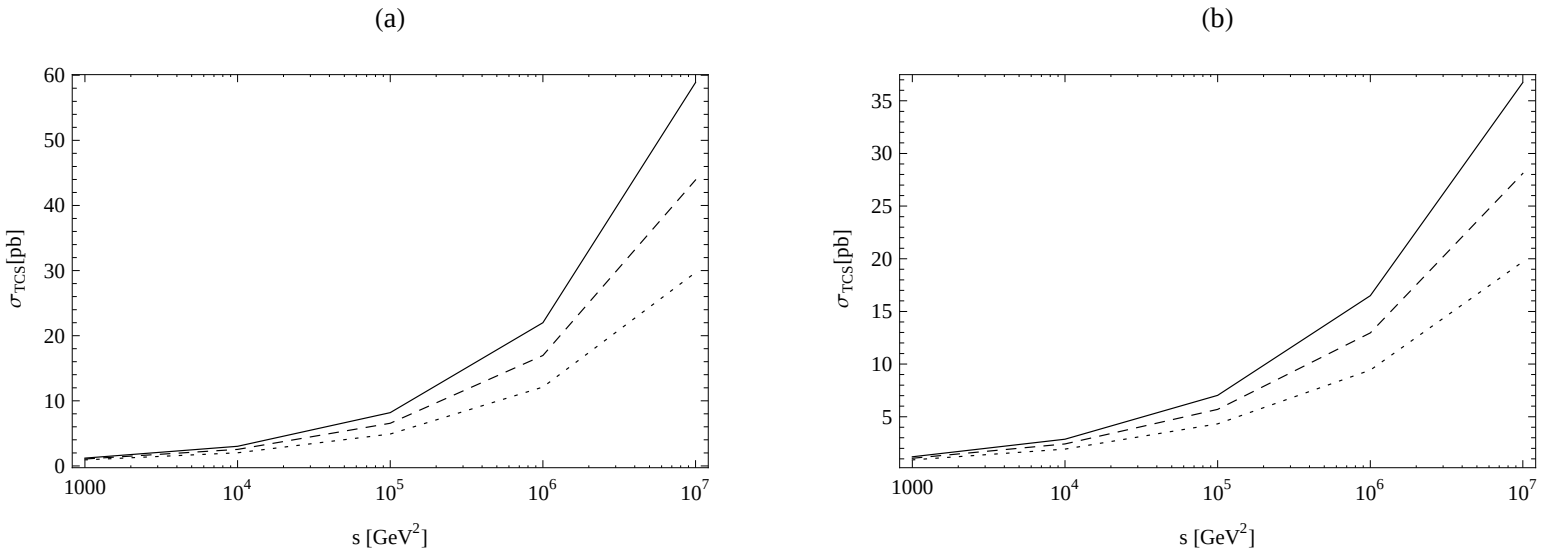

Figure: σ_{TCS} as a function of γp c.m. energy squared s, for GRVGJR2008 LO (a) and NLO (b) parametrizations, for different factorization scales $\mu_F^2 = 4$ (dotted), 5 (dashed), 6 (solid) GeV^2.

For very high energies σ_{TCS} calculated with $\mu_F^2 = 6\,\mathrm{GeV}^2$ is much bigger then with $\mu_F^2 = 4\,\mathrm{GeV}^2$. Also predictions obtained using LO and NLO GRVGJR2008 PDFs differ significantly.

The interference cross section

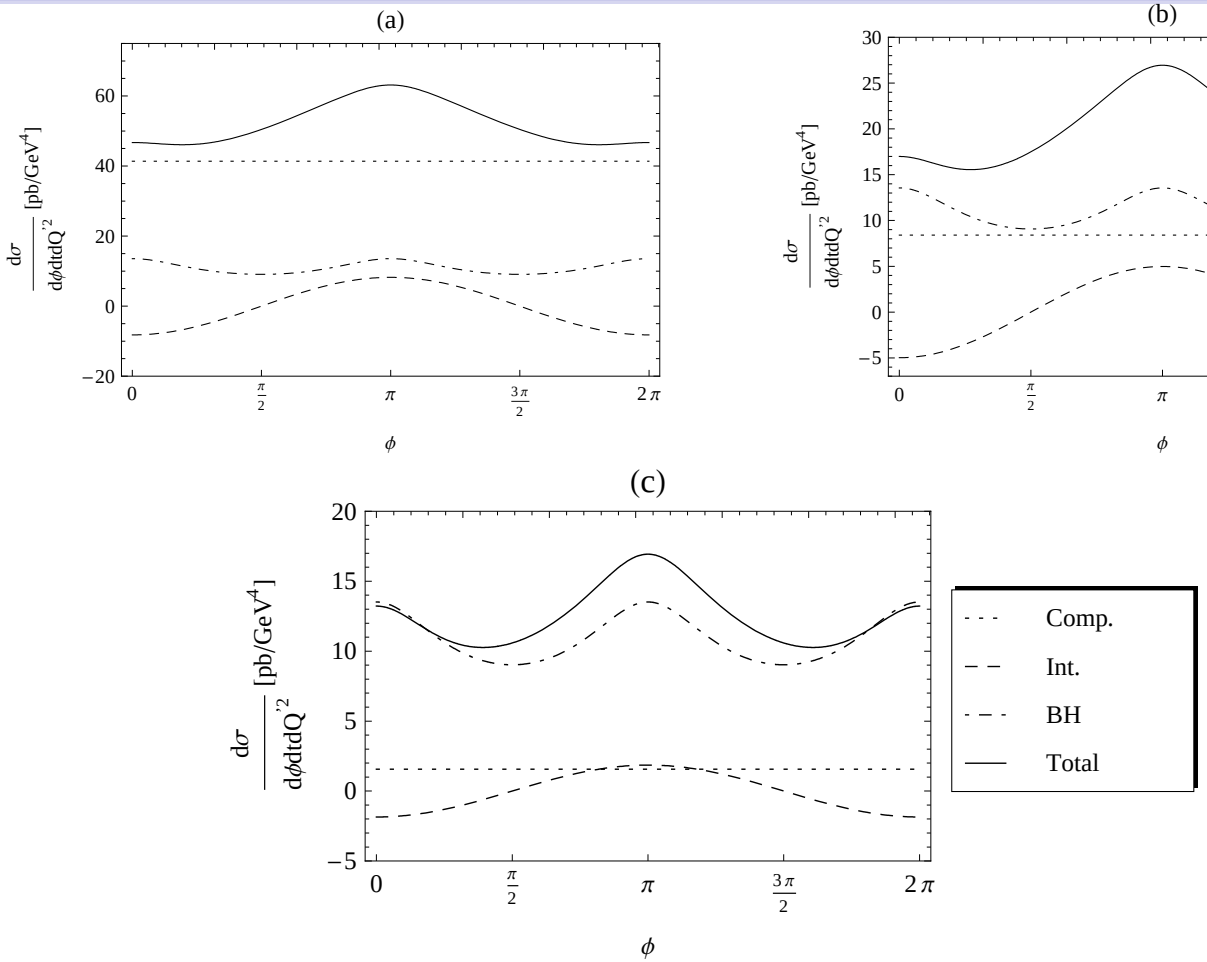

Figure: The differential cross sections (solid lines) for $t = -0.2\,\mathrm{GeV}^2$, $Q'^2 = 5\,\mathrm{GeV}^2$ and integrated over $\theta = [\pi/4, 3\pi/4]$, as a function of φ, for $s = 10^7\,\mathrm{GeV}^2$ (a), $s = 10^5\,\mathrm{GeV}^2$(b), $s = 10^3\,\mathrm{GeV}^2$ (c) with $\mu_F^2 = 5\,\mathrm{GeV}^2$. We also display the Compton (dotted), Bethe-Heitler (dash-dotted) and Interference (dashed) contributions.

Motivation for NLO

Why do we need NLO corrections to TCS:

- at high energies gluons important, they enter at NLO
- DIS versus Drell-Yan: big K-factors $\log \frac{-Q^2}{\mu_F^2} \to \log \frac{Q^2}{\mu_F^2} \pm i\pi$
- dependence on the factorization scale μ_F

TCS, DVCS, DDVCS in one framework

$$\gamma^*(q_{in})N \to \gamma^*(q_{out})N'$$

DVCS versus TCS versus DDVCS:

- DVCS: $q_{in}^2 < 0\,, \quad q_{out}^2 = 0$
- TCS: $q_{in}^2 = 0\,, \quad q_{out}^2 > 0$
- DDVCS: $q_{in}^2 < 0\,, \quad q_{out}^2 > 0$

Amplitude:

$$\mathcal{A}^{\mu\nu} = g_T^{\mu\nu} \int_{-1}^{1} dx \left[\sum_q^{n_F} T^q(x) F^q(x) + T^g(x) F^g(x) \right]$$

where renormalized coefficient functions are given by:

$$\begin{aligned} T^q &= C_0^q + C_1^q + \frac{1}{2} \ln\left(\frac{|Q^2|}{\mu_F^2}\right) \cdot C_{coll}^q \,, \\ T^g &= C_1^g + \frac{1}{2} \ln\left(\frac{|Q^2|}{\mu_F^2}\right) \cdot C_{coll}^g \end{aligned}$$

and the GPDs are

$$\begin{aligned} F^q(x,\xi) &= \frac{1}{2} \int \frac{d\lambda}{2\pi} e^{-i\lambda x} \left\langle P' \middle| \bar{\psi}_q\left(\frac{\lambda}{2} n\right) \gamma^\mu \psi_q\left(-\frac{\lambda}{2} n\right) \middle| P \right\rangle n_\mu \,, \\ F^g(x,\xi) &= -\frac{1}{2x} \int \frac{d\lambda}{2\pi} e^{-i\lambda x} \left\langle P' \middle| F_a^{\mu\alpha}\left(\frac{\lambda}{2} n\right) F_{a\alpha}^{\nu}\left(-\frac{\lambda}{2} n\right) \middle| P \right\rangle n_\mu n_\nu \end{aligned}$$

Diagrams

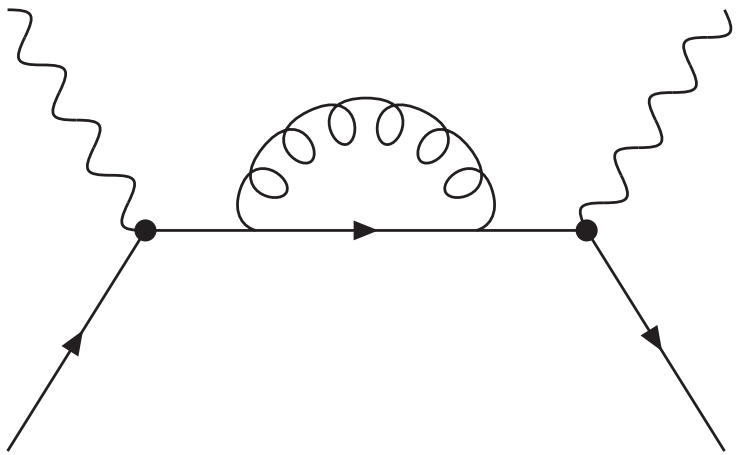

Figure: Self energy correction to $q\gamma \to q\gamma$ scattering amplitude

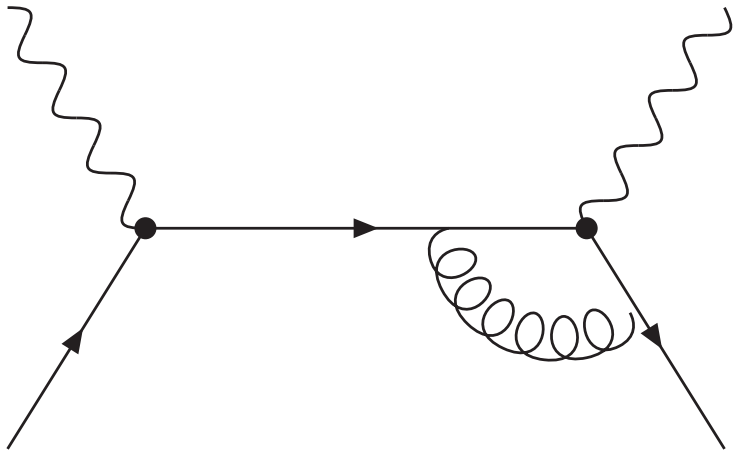

Figure: Right vertex correction to $q\gamma \to q\gamma$ scattering amplitude

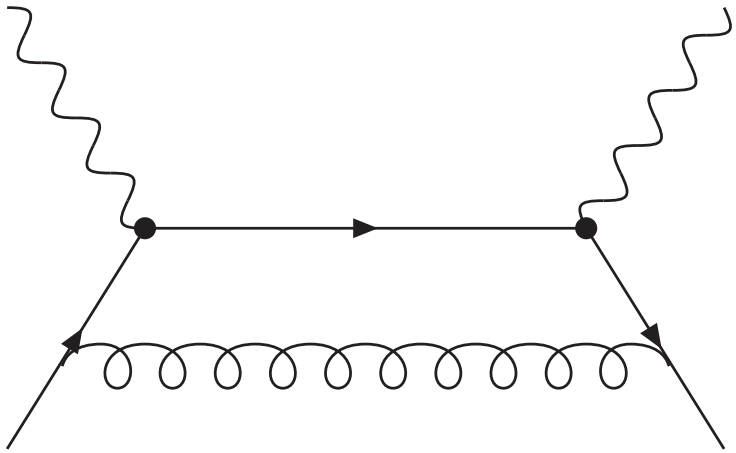

Figure: Box diagram correction to $q\gamma \to q\gamma$ scaterring amplitude

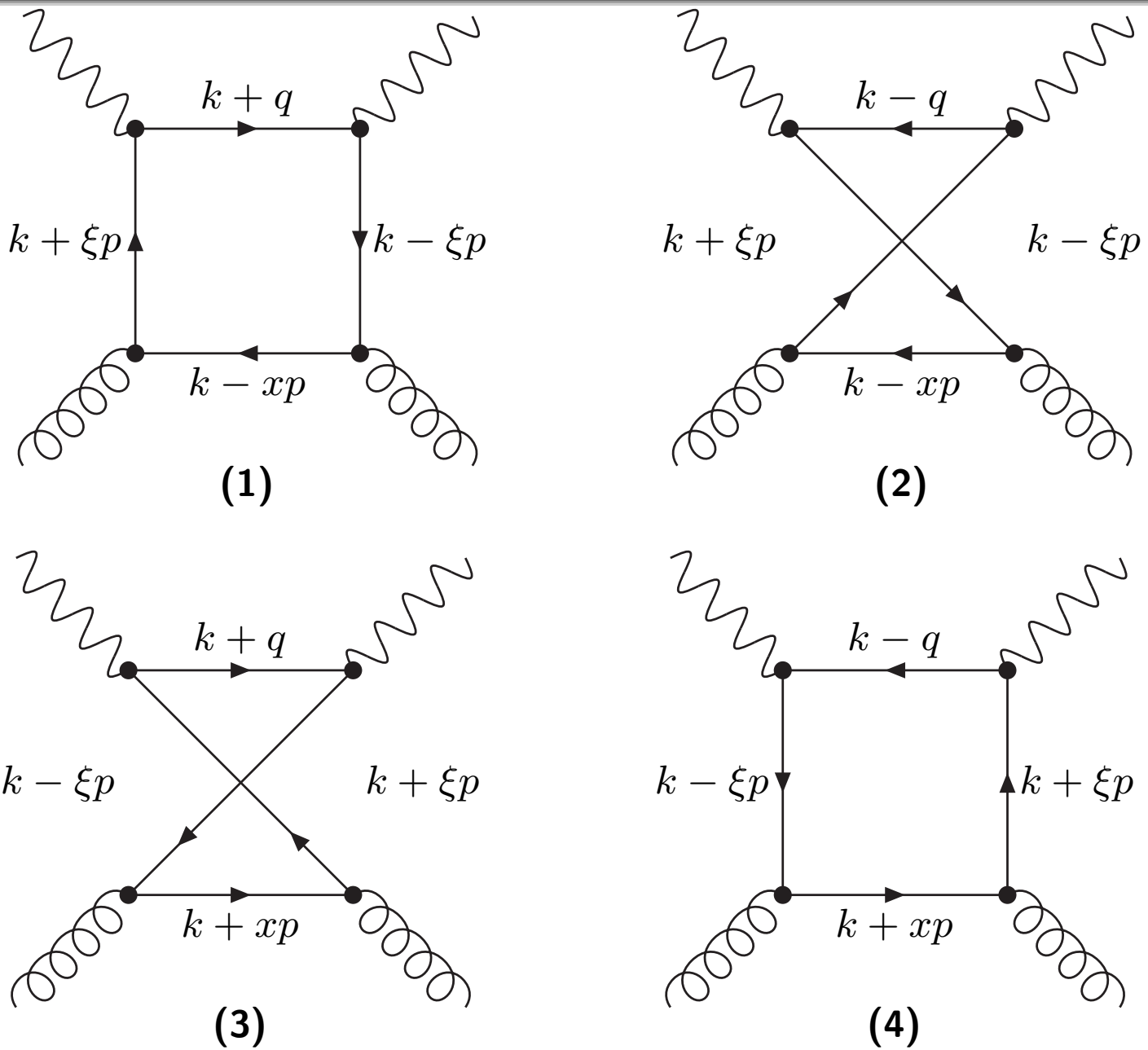

Figure: First group of diagrams describing $\gamma g \to \gamma g$ scattering.

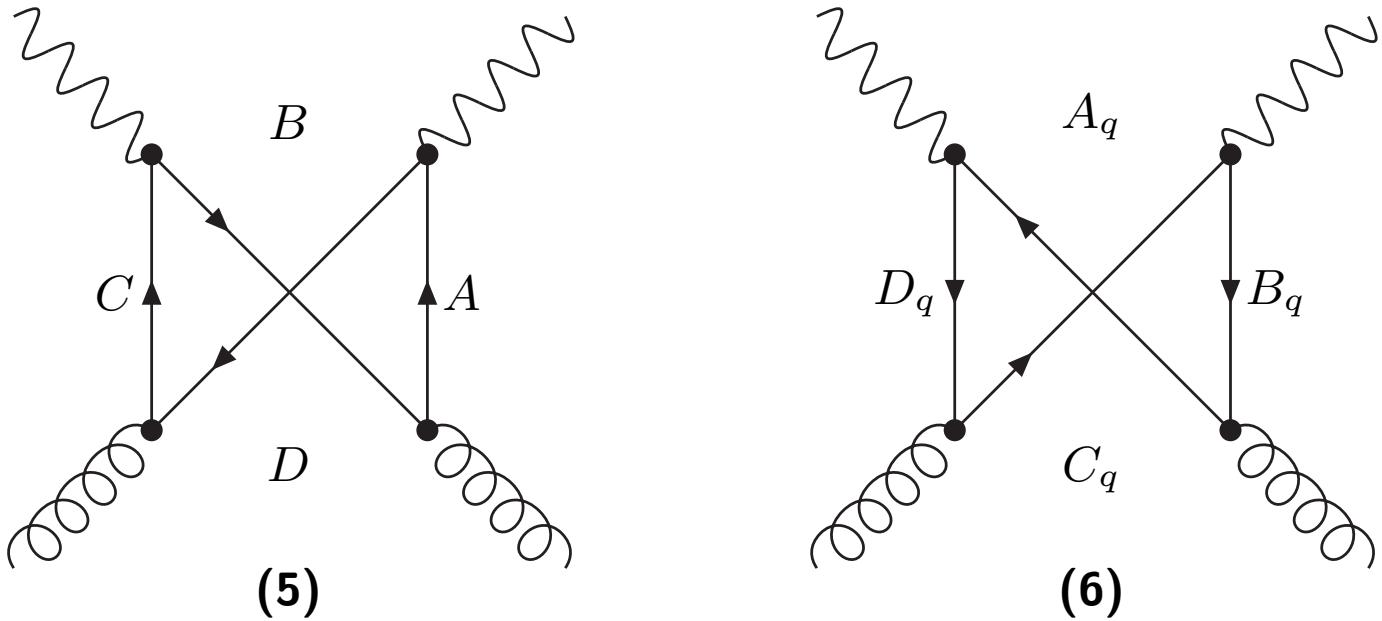

Figure: Second group of diagrams describing $\gamma g \to \gamma g$ scattering.

Results: TCS + DVCS + DDVCS

TCS:

Quark coefficient functions:

$$C_0^q = e_q^2 \left(\frac{1}{x-\xi-i\varepsilon} + \frac{1}{x+\xi+i\varepsilon} \right) ,$$

$$C_1^q = \frac{e_q^2 \alpha_S C_F}{4\pi}$$

$$\left\{ \frac{1}{x-\xi-i\varepsilon} \left[-9 + 3\log(-1+\frac{x}{\xi}-i\varepsilon) - 6\frac{\xi}{x+\xi}\log(-1+\frac{x}{\xi}-i\varepsilon) + 6\frac{\xi}{x+\xi}\log(-2-i\varepsilon) \right.\right.$$
$$\left. + \log^2(-1+\frac{x}{\xi}-i\varepsilon) - \log^2(-2-i\varepsilon) \right]$$
$$+ \frac{1}{x+\xi+i\varepsilon} \left[-9 + 3\log(-1-\frac{x}{\xi}-i\varepsilon) + 6\frac{\xi}{x-\xi}\log(-1-\frac{x}{\xi}-i\varepsilon) - 6\frac{\xi}{x-\xi}\log(-2-i\varepsilon) \right.$$
$$\left.\left. + \log^2(-1-\frac{x}{\xi}-i\varepsilon) - \log^2(-2-i\varepsilon) \right] \right\} ,$$

$$C_{coll}^q = \frac{e_q^2 \alpha_S C_F}{4\pi} \left\{ \frac{1}{x-\xi-i\varepsilon} \left[6 + 4\log(-1+\frac{x}{\xi}-i\varepsilon) - 4\log(-2-i\varepsilon) \right] \right.$$
$$\left. + \frac{1}{x+\xi+i\varepsilon} \left[6 + 4\log(-1-\frac{x}{\xi}-i\varepsilon) - 4\log(-2-i\varepsilon) \right] \right\}$$

Gluon coefficient functions:

$$C^g_{coll} = \frac{\left(\sum_q e_q^2\right)\alpha_S T_F}{4\pi}\frac{8x}{(x+\xi+i\varepsilon)(x-\xi-i\varepsilon)}\cdot$$
$$\left[\frac{x-\xi}{x+\xi}\log\left(-1+\frac{x}{\xi}-i\varepsilon\right)+\frac{x+\xi}{x-\xi}\log\left(-1-\frac{x}{\xi}-i\varepsilon\right)-2\frac{x^2+\xi^2}{x^2-\xi^2}\log(-2-i\varepsilon)\right],$$

$$C^g_1 = \frac{\left(\sum_q e_q^2\right)\alpha_S T_F}{4\pi}\frac{2x}{(x+\xi+i\varepsilon)(x-\xi-i\varepsilon)}\cdot$$
$$\left[-2\frac{x-3\xi}{x+\xi}\log\left(-1+\frac{x}{\xi}-i\varepsilon\right)+\frac{x-\xi}{x+\xi}\log^2\left(-1+\frac{x}{\xi}-i\varepsilon\right)\right.$$
$$-2\frac{x+3\xi}{x-\xi}\log\left(-1-\frac{x}{\xi}-i\varepsilon\right)+\frac{x+\xi}{x-\xi}\log^2\left(-1-\frac{x}{\xi}-i\varepsilon\right)$$
$$\left.+4\frac{x^2+3\xi^2}{x^2-\xi^2}\log(-2-i\varepsilon)-2\frac{x^2+\xi^2}{x^2-\xi^2}\log^2(-2-i\varepsilon)\right]$$

Discussion

- DVCS: the imaginary parts from $\xi \longrightarrow \xi - i\varepsilon$
- TCS:
  - part of imaginary parts from $\xi \longrightarrow \xi + i\varepsilon$
  - there appear e.g. $\log^2(-2 - i\varepsilon)$ which contribute to imaginary parts
  - in DVCS the imaginary part are in DGLAP region
    in TCS they are in DGLAP AND ERBL
- at LO: $C^q_{0(DVCS)} = {C^q_{0(TCS)}}^*$

  at NLO: $C^q_{coll(DVCS)} = {C^q_{coll(TCS)}}^*$ and $C^g_{coll(DVCS)} = {C^g_{coll(TCS)}}^*$

NLO quark:

$$\frac{{C^q_{1(TCS)}}^* - C^q_{1(DVCS)}}{\frac{e^2\alpha_S C_F}{4\pi}} =$$

$$\frac{1}{x-\xi+i\varepsilon}\left[\left(3-2\log 2+2\log|1-\frac{x}{\xi}|\right)(i\pi)+\pi^2\left(1+\theta(x-\xi)-\theta(-x+\xi)\right)\right]$$

$$+\frac{1}{x+\xi-i\varepsilon}\left[\left(3-2\log 2+2\log|1+\frac{x}{\xi}|\right)(i\pi)+\pi^2\left(1+\theta(-x-\xi)-\theta(x+\xi)\right)\right]$$

NLO gluon in DGLAP region:

$$\frac{C^g_{1(TCS)} - C^g_{1(DVCS)}}{\frac{\left(\sum_q e_q^2\right)\alpha_S T_F}{4\pi}} \overset{x\geq\xi}{=} \frac{2x}{x^2-\xi^2}\left[2\frac{x-\xi}{x+\xi}\pi^2\right.$$

$$\left.+\left(-4\frac{x-3\xi}{x+\xi}+2\frac{x-\xi}{x+\xi}\log|1-\frac{x}{\xi}|-2\frac{x+\xi}{x-\xi}\log|1+\frac{x}{\xi}|+4\frac{x^2+\xi^2}{x^2-\xi^2}\log 2\right)(-i\pi)\right]$$

$$\text{quark ratio:} \quad R^q = \frac{C_1^q + \frac{1}{2}\log\left(\frac{|Q^2|}{\mu_F^2}\right) \cdot C_{coll}^q}{C_0^q}$$

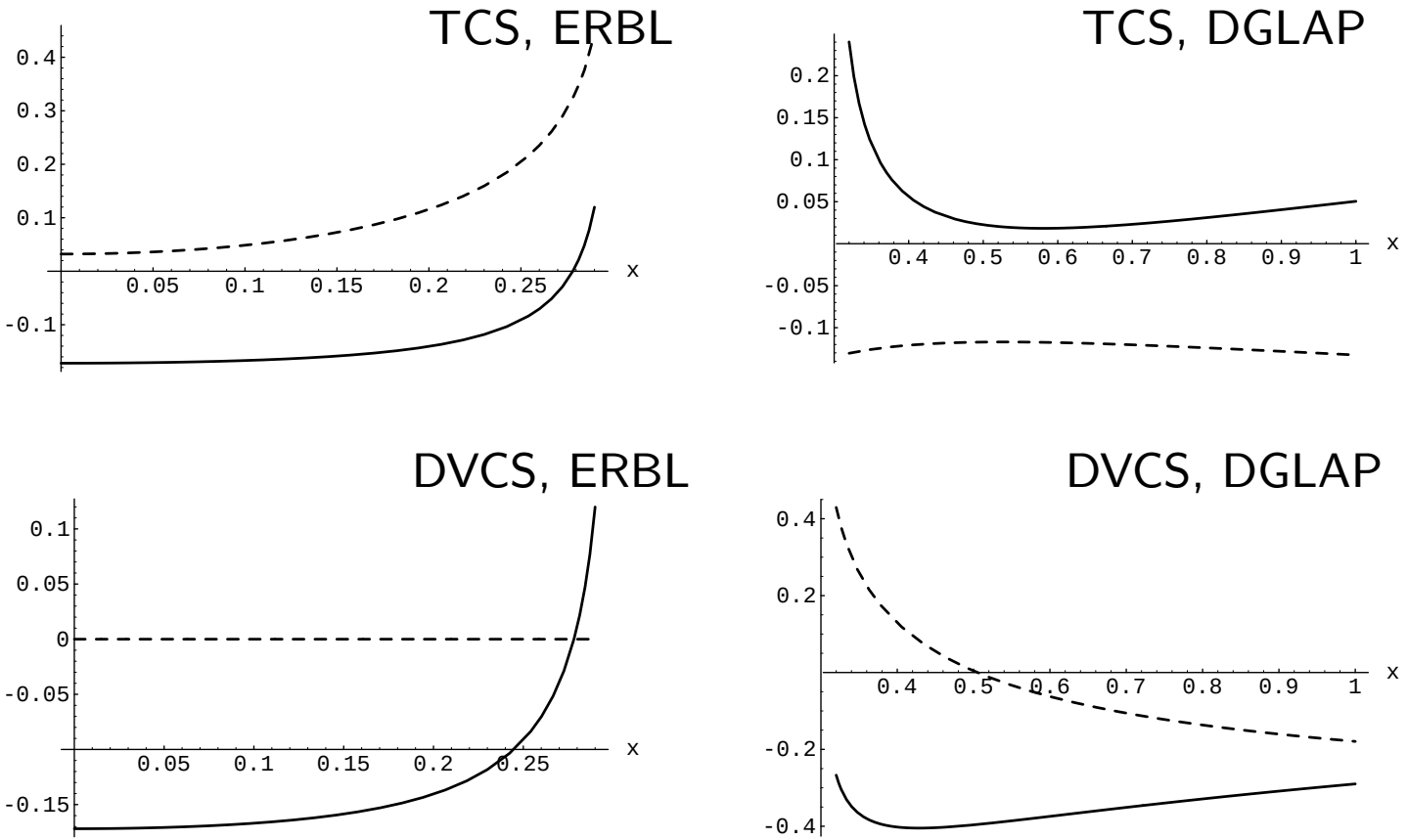

Figure: Real (solid line) and imaginary (dashed line) part of the ratio R^q of the NLO quark coefficient function to the Born term in Timelike Compton Scattering (up) and Deeply Virtual Compton Scattering (down) as a function of x in the ERBL (left) and DGLAP (right) region for $\xi = 0.3$, for $\mu_F^2 = |Q^2|$.

another quark ratio: $R^q_{T-S} = \dfrac{C^q_{1(TCS)} - C^{q\,*}_{1(DVCS)}}{C^q_0}$

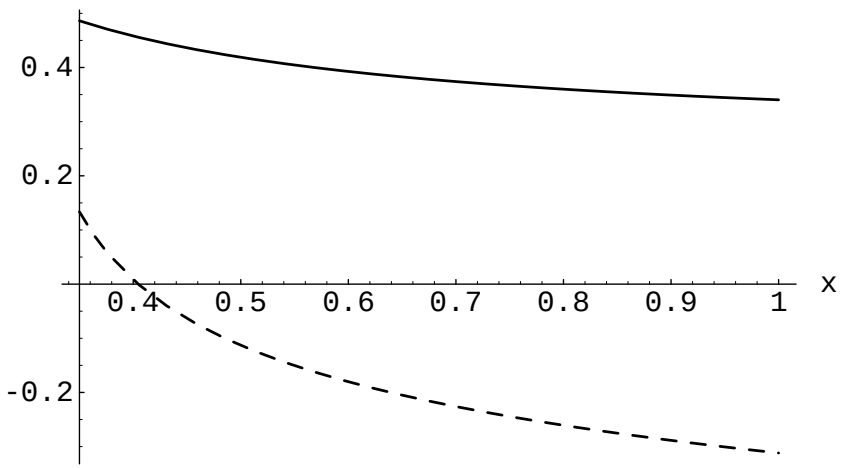

Figure: Real (solid line) and imaginary (dashed line) part of the ratio R^q_{T-S} of difference of NLO quark coefficient functions to the LO coefficient functions in the TCS and DVCS as a function of x in the DGLAP region for $\xi = 0.3$.

gluonic ratios:

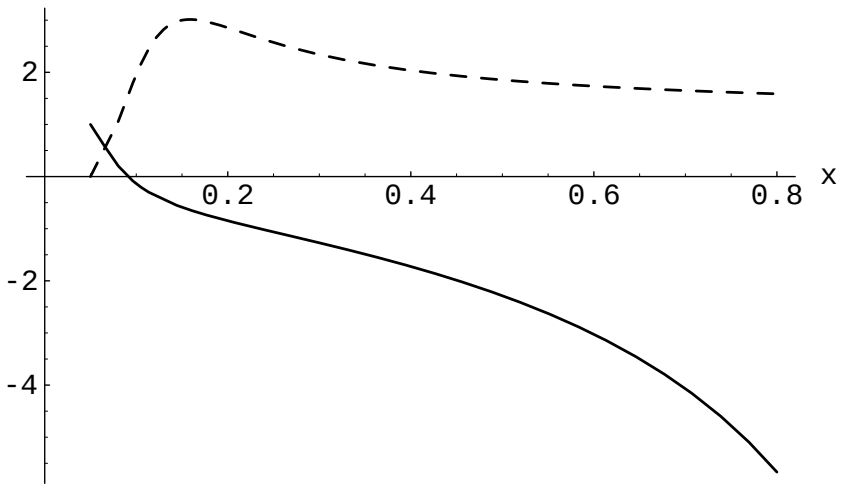

Figure: Ratio of the real (solid line) and imaginary (dashed line) part of the NLO gluon coefficient function in TCS to the same quantity in DVCS as a function of x in the DGLAP region for $\xi = 0.05$ for $\mu_F^2 = |Q^2|$.

DVCS Compton Form Factors at NLO

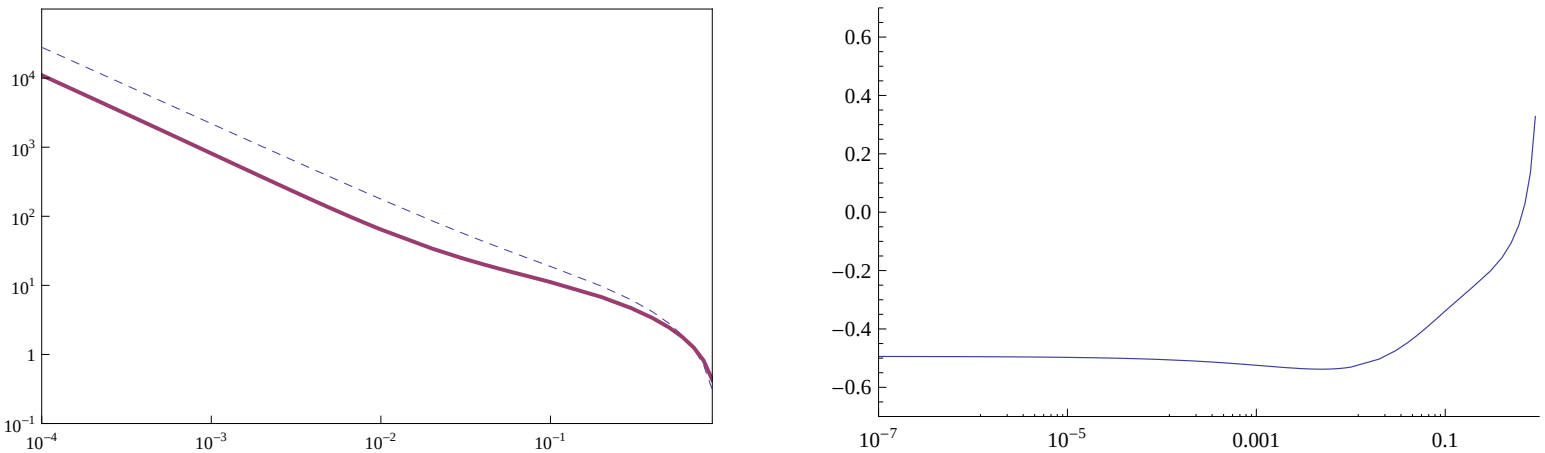

Figure: (left) Imaginary part of the DVCS Compton Form Factor $\mathcal{H}$, in the LO (dashed) and NLO (solid). (right) Ratio of the NLO corection to the Born term for imaginary part of the Compton Form Factor $\mathcal{H}$. Calculated for Kroll-Goloskokov model with $t = -0.1\ \mathrm{GeV}^2, Q^2 = 5\ \mathrm{GeV}^2$.

In collaboration with H.Moutarde and F.Sabatie from CEA, Saclay

TCS Compton Form Factors at NLO

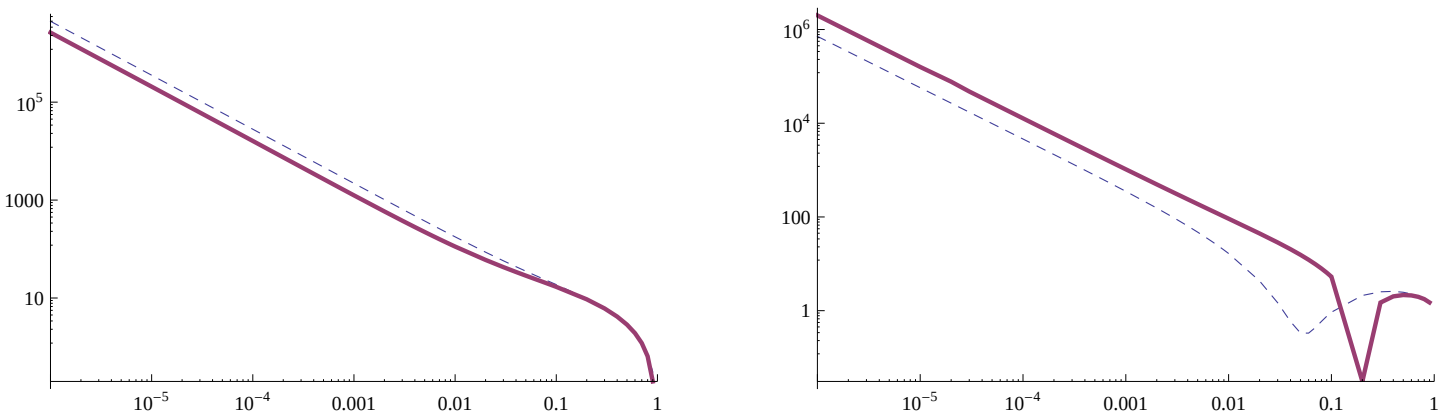

Figure: (left) Absolute value of the imaginary part of the TCS Compton Form Factor $\mathcal{H}$, in the LO (dashed) and NLO (solid). (right) Absolute value of the real part of the TCS Compton Form Factor $\mathcal{H}$, in the LO (dashed) and NLO (solid). Calculated for Kroll-Goloskokov model with $t = -0.1\ \mathrm{GeV}^2, Q^2 = 5\ \mathrm{GeV}^2$.

TCS Compton Form Factors at NLO

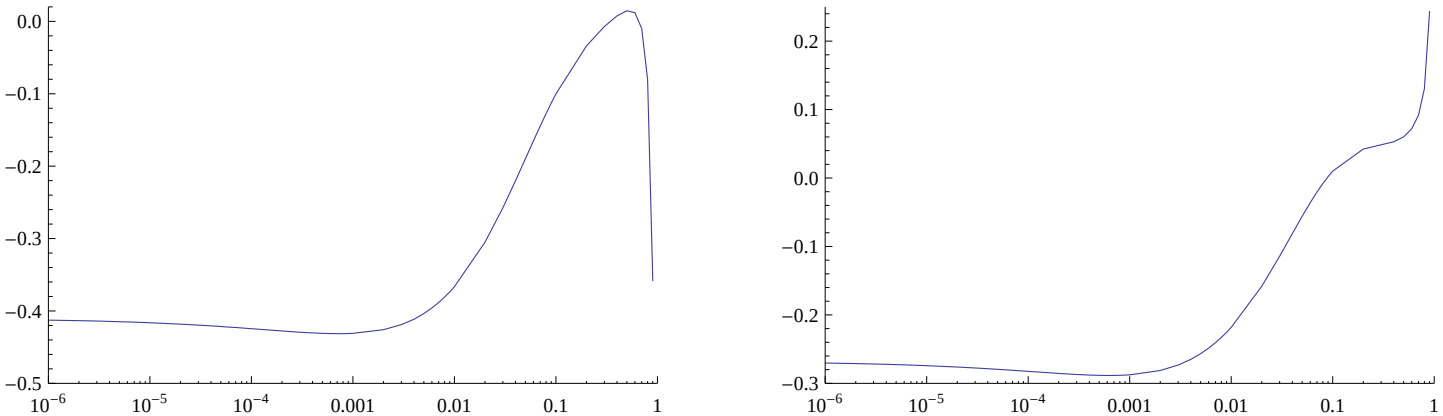

Figure: (left)Ratio of the NLO correction to the Born term for the imaginary part of CFF $\mathcal{H}$. (right)Gluon contribution to that ratio.

TCS Compton Form Factors at NLO

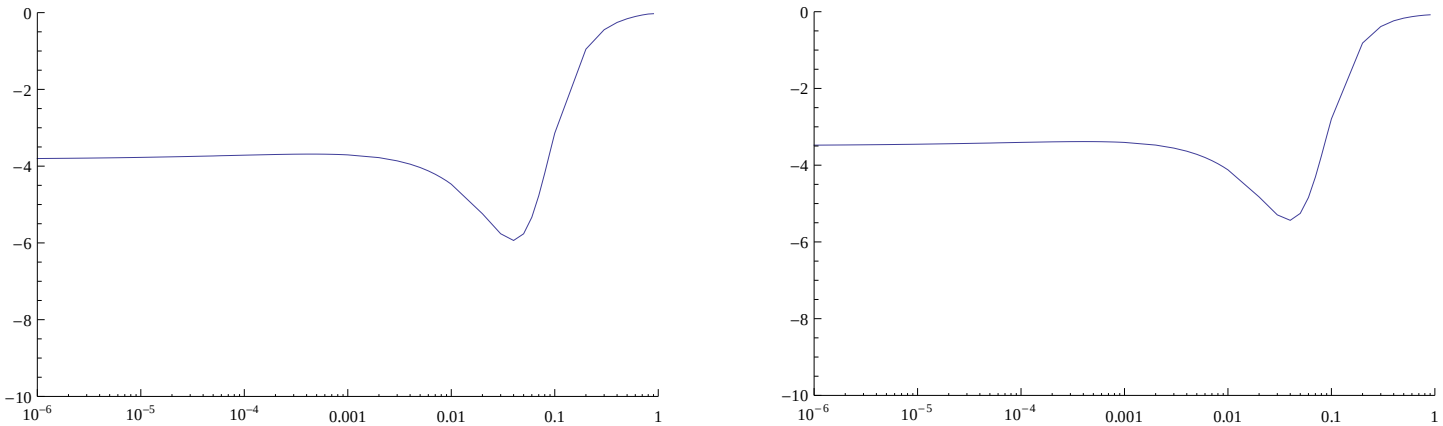

Figure: (left)Ratio of the NLO correction to the Born term for the real part of CFF $\mathcal{H}$. (right)Gluon contribution to that ratio.

Ultraperipheral collisions

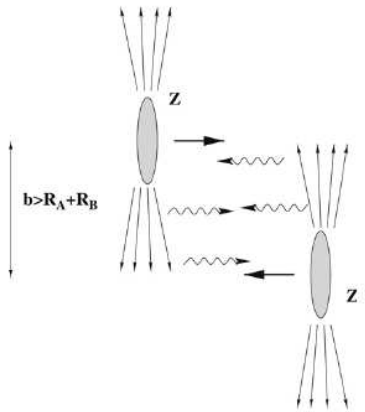

$$\sigma_{pp} = 2 \int \frac{dn(k)}{dk} \sigma_{\gamma p}(k) dk$$

$\sigma_{\gamma p}(k)$ is the cross section for the $\gamma p \to p l^+ l^-$ process and k is the γ's energy.

$\frac{dn(k)}{dk}$ is an equivalent photon flux

$$\frac{dn(k)}{dk} = \frac{\alpha}{2\pi k} \left[1 + (1 - \frac{2k}{\sqrt{s_{pp}}})^2 \right] \left(\ln A - \frac{11}{6} + \frac{3}{A} - \frac{3}{2A^2} + \frac{1}{3A^3} \right)$$

$A = 1 + \frac{0.71\,\mathrm{GeV}^2}{Q^2_{min}}$, $Q^2_{min} \approx \frac{4M_p^2 k^2}{s_{pp}}$ is the minimal $-t$

s_{pp} is the proton-proton energy squared ($\sqrt{s_{pp}} = 14\,\mathrm{TeV}$): $s \approx 2\sqrt{s_{pp}} k$

UPC Rate estimates

The pure Bethe - Heitler contribution to σ_{pp}, integrated over $\theta = [\pi/4, 3\pi/4]$, $\phi = [0, 2\pi]$, $t = [-0.05\,\mathrm{GeV}^2, -0.25\,\mathrm{GeV}^2]$, $Q'^2 = [4.5\,\mathrm{GeV}^2, 5.5\,\mathrm{GeV}^2]$, and photon energies $k = [20, 900]\,\mathrm{GeV}$ gives:

$$\sigma_{pp}^{BH} = 2.9\mathrm{pb}\ .$$

The Compton contribution gives:

$$\sigma_{pp}^{TCS} = 1.9\mathrm{pb}\ .$$

LHC: rate $\sim 10^5$ events/year with nominal luminosity $(10^{34}\,\mathrm{cm}^{-2}\mathrm{s}^{-1})$

Ultrperipheral collisions at RHIC

$$L \cdot k \frac{dn}{dk} (\mathrm{mb}^{-1} \mathrm{sec}^{-1})$$

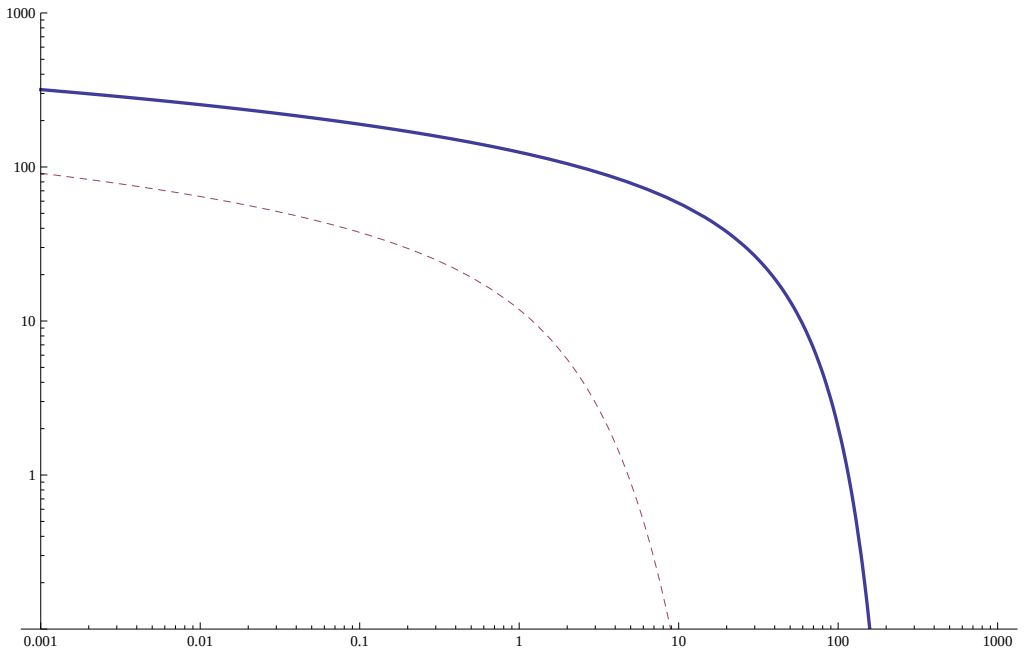

Figure: Effective luminosity of the photon flux from the Au-Au (dashed) and proton-proton (solid) collisions as a function of photon energy k(GeV).

RHIC

$\frac{d\sigma^{AuAu}}{dQ^2 dt d\phi}(\mu\text{b GeV}^{-4})$

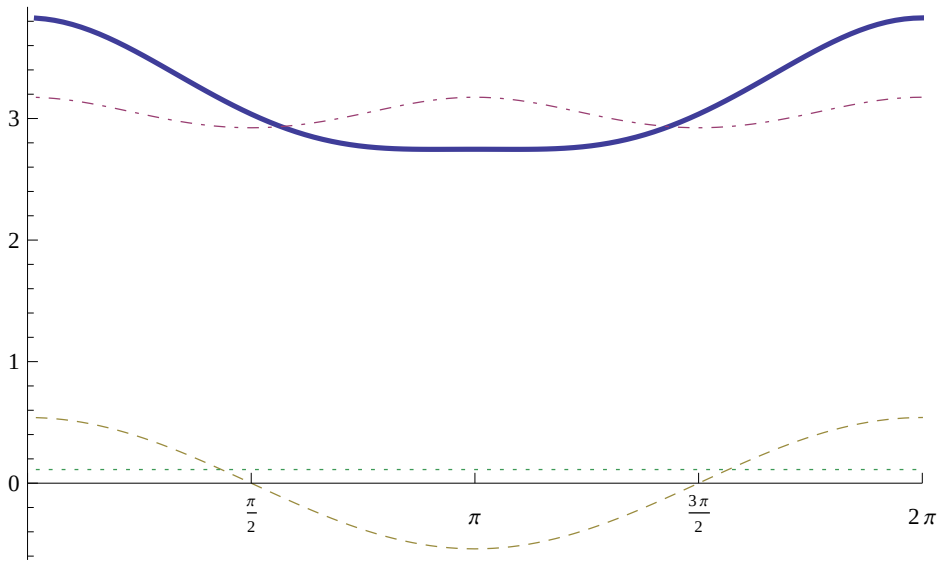

Figure: The differential cross sections (solid lines) for $t = -0.1\,\text{GeV}^2$, $Q'^2 = 5\,\text{GeV}^2$ and integrated over $\theta = [\pi/4, 3\pi/4]$, as a function of φ. We also display the Compton (dotted), Bethe-Heitler (dash-dotted) and Interference (dashed) contributions.

Total BH cross section (for $Q \in (2, 2.9)\,\text{GeV}$, $t \in (-0.2, -0.05)\,\text{GeV}^2$, $\theta = [\pi/4, 3\pi/4]$ and $\phi \in (0, 2\pi)$)

$$\sigma_{BH} = 41\mu\text{b} \qquad \text{Rate} = 0.04\text{Hz}$$

RHIC

$\frac{d\sigma^{pp}}{dQ^2 dt d\phi}(\text{pb GeV}^{-4})$

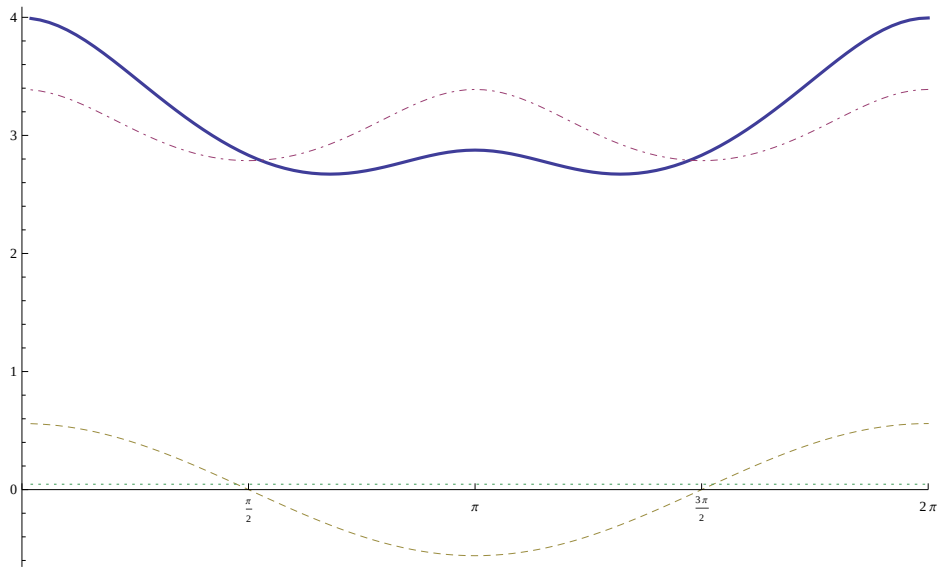

Figure: The differential cross sections (solid lines) for $t = -0.1\,\text{GeV}^2$, $Q'^2 = 5\,\text{GeV}^2$ and integrated over $\theta = [\pi/4, 3\pi/4]$, as a function of φ. We also display the Compton (dotted), Bethe-Heitler (dash-dotted) and Interference (dashed) contributions.

Total BH cross section (for $Q \in (2, 2.9)\,\text{GeV}$, $t \in (-0.2, -0.05)\,\text{GeV}^2$, $\theta = [\pi/4, 3\pi/4]$ and $\phi \in (0, 2\pi)$)

$$\sigma_{BH} = 9\text{pb} \qquad \text{Rate} = 5/\text{day}$$

Summary

- GDPs enter factorization theorems for hard exlusive reactions (DVCS, deeply virtual meson production etc.), in a similar manner as PDFs enter factorization theorem for DIS
- First moment of GPDs enter the Ji's sum rule for the angular momentum carried by partons in the nucleon.
- Fourier transform of GPD's to impact parameter space can be interpreted as „tomographic" 3D pictures of nucleon, describing charge distribution in the transverse plane, for a given value of x.
- Compton scattering in ultraperipheral collisions at hadron colliders opens a new way to measure generalized parton distributions.
- Measurable rates for Au-Au and p-p collisions at RHIC.
- Big NLO corrections from gluon sector,
- better understanding of large terms (π^2, ??) is needed resummation ??